ORIGINAL SCIENTIFIC PAPER

CROATICA CHEMICA ACTA

Croat. Chem. Acta **2026**, *99*(2), 175–183
Published online: June 28, 2026
DOI: 10.5562/cca4247

HKD 1926

DFT Approach to the Gibbs Energy of Hydride Anion in Acetonitrile by Modelling Hydricities

Zoran Glasovac,[1,*] Borislav Kovačević,[2] Davor Margetić[1]

[1] Ruđer Bošković Institute, Division of organic chemistry and biochemistry, Bijenička c. 54, 10000, Zagreb, Croatia

[2] Ruđer Bošković Institute, Division of physical chemistry, Bijenička c. 54, 10000, Zagreb, Croatia

* Corresponding author's e-mail address: glasovac@irb.hr

RECEIVED: January 19, 2026 * REVISED: May 15, 2026 * ACCEPTED: May 20, 2026

Abstract: Hydricity values for a range of non-metallic hydride donors were calculated using 25 different computational approaches, which included various density functionals and continuum solvent models. The quality of these results was assessed by comparing the computed data to experimental values, focusing on the correlation and deviation between them. The B2PLYP–D3 / CPCM-based methods demonstrated the best performance with ωB97xD / CPCM being only marginally behind. All methods show minimal influence from the size of the basis set, with correlations with correlation coefficients (r^2) of 0.994 or higher. Comparable results were obtained whether the structures were optimized in the gas phase or in solution. The most significant errors were noted for borohydride derivatives. The correlation data were used to estimate the Gibbs energy of the hydride anion in acetonitrile ($G^*(H^-)$). The estimated value of –403.1 kcal mol^{-1} aligns well with the literature data.
.

Keywords: hydricity, DFT calculations, continuum solvation models, Gibbs energy, hydride anion.

INTRODUCTION

REDUCTION is one of the fundamental organic reactions, and a variety of reagents have been developed to react with a broad scope of substrates.[1] The most common laboratory reductants, such as borohydrides and aluminohydrides, are donors of hydride anion to the electrophilic center in the substrate, for example, the carbon atom of the carbonyl group, leading to the desired reduced product. Many reductions were performed using gaseous hydrogen with rare metal complexes as catalysts. The catalytic cycle involves switching between different oxidation states of the metal atom associated with in situ conversion to hydride and subsequent hydride transfer to the substrate.[2–4] Another important group of hydrides comprises bioinspired organic hydride donors such as NADH and Hantzsch esters.[5,6] While these compounds are attractive due to their low cost and absence of potentially toxic transition metals or expensive rare-earth metals, they are usually used in stochiometric quantities, and their regeneration is typically cumbersome. Nevertheless, the demands of modern chemistry for sustainable processes, combined with the urgency of addressing the global warming problem, have made the organic hydrides a subject of many investigations, especially in the context of CO_2 reduction.[6,7]

The thermodynamic quantities that describe the ability of donors to transfer the hydride anion to the substrate are hydricity and hydride affinity, and they are related to the Gibbs energy or enthalpy of the reaction given in Eq. (1).[8–10]

$$BH^{[0/-]} \rightarrow BH^{[+/0]} + H^- \qquad (1)$$

It should be emphasized that the hydricity is defined as the property of the Lewis base BH^0 or BH^- ($\Delta G°_H$-($BH^{[0/-]}$) = $\Delta_r G°(1)$), while the hydride affinity (HA) is defined as the property of the Lewis acid BH^+ or B (HA($B^{[+/0]}$) = $\Delta_r H°(1)$), depending on the nature of the hydride donor.

It is clear that the efficacy of the hydride transfer depends on the difference in hydricity of the hydride donor and the product. Most of the data published nowadays are thermodynamic hydricities obtained from measuring the

This work is licensed under a Creative Commons Attribution 4.0 International License.

equilibrium constants. The proven capability of these data to predict the reactivity emphasized their importance and triggered interest among computational chemists.[8,11] To date, many computational data on hydricity determination for a variety of hydride donors have been published, complementing experimental measurements and expanding the pool of potential hydride donors.[12–15] We found it particularly intriguing that the excellent correlations were obtained by employing markedly different functionals, B3LYP(PCM = ACN) / 6–31 + G(d,p), where the cavity was constructed using UAHF radii[12] and ωB97xD(CPCM = ACN) / 6–31 + G(d,p) with UFF radii alone or complemented with ωB97xD(CPCM = ACN) / def2-TZVP calculations of the electronic energies[15]. The ωB97xD–based models were benchmarked on a relatively small dataset, and the comparison showed a better linear fit when a small basis set was used for the hydricity calculations. The Muckermann's approach[15], subsequently used by Glusac and coworkers,[13] provided a very good correlation for numerous hydricity values. Both approaches are based on the linear correlation between experimental hydricities and "Hydricity half reaction ($\Delta G^*_{HHR}(AH^-)$)" followed by further correction of the data using the derived linear function. This approach is essentially the same as the one we have used to calculate pK_a in acetonitrile,[16,17] where their $\Delta G^*_{HHR}(AH^-)$ is analogous to our "reduced basicity". In this way, uncertainties and errors in determining the Gibbs energy of proton and hydride in the particular solvents, as well as the need for a specific reference value, are avoided.

We are continuously looking for simple computational models that can predict properties of organic molecules with sufficient accuracy and without needing any specific reference system to anchor the results. An important obstacle is the systematic error inherent in the implicit solvation models.[18,19] Nevertheless, very good results are typically achieved by linear correlation–based approaches like those mentioned above.[12,15,17] In one of our preceding papers, we have presented a procedure to estimate the Gibbs energy of a proton in a given solvent – a value typically obscured by the systematic error in computations.[17] The same logic can be applied here, and in this work, we are using several computational models to estimate the Gibbs energy of the hydride ion in acetonitrile and to analyze the influence of the basis set, solvation model, and different DFT functionals on the quality of the correlations between the experimental and computed data. Since all hydricity data found in the literature are given in kcal mol^{-1}, the same unit will be used in this work (1 kcal mol^{-1} = 4.184 kJ mol^{-1}).

Computational Methods

All computations were performed using the Gaussian16 program package[20] with default optimization and the SCF energy convergence criteria. All minima at the potential energy surface have been confirmed by vibrational analysis (NImag=0). Gibbs energies were calculated at 298 K using unscaled frequencies. The geometry optimizations were conducted using three different density functionals with different degrees of the dispersion correction included: ωB97xD,[21] M06–2X[22] and B3LYP.[23–26] For this purpose, a double-ζ quality basis sets were used (see list of models given below). The same functionals were also employed in single-point energy calculations in combination with triple-ζ quality basis sets, and their performance was tested against B2PLYP–D3[28,29] and MP2[30,31] methods. The role of the dispersion was checked with models M15 and M16 where GD3 empirical dispersion[27] was included atop the B3LYP approach. Structures were optimized either in solution by using CPCM [32,33] or SMD [34] continuum solvation models or in the gas phase. In the latter case, the IPCM [35] model was also taken into consideration, and the solvation energies were added to the gas phase Gibbs energy for each species according to Eq. (2):

$$G(\mathrm{B})_{\mathrm{ACN}} = G(\mathrm{B})_{\mathrm{gas}} + E_{\mathrm{scf}}(\mathrm{B})_{\mathrm{SM,\,ACN}} - E_{\mathrm{scf}}(\mathrm{B})_{\mathrm{SM,\,gas}} \qquad (2)$$

Within the CPCM and SMD models, the dielectric constant for acetonitrile was used as implemented (ε = 35.688), whereas for the IPCM, it was set to 36.64. Additional non-standard parameters within the IPCM model were as follows: the isodensity parameter for the molecular cavities in solution embracing the solute molecule was 4×10^{-4}, and the angular integration weights over polar coordinates ϑ and φ were set to 100 and 20, respectively.

Employed models are listed below.

M1 = CPCM(ACN)/ωB97xD/6-31+G(d,p)
M2 = CPCM (CAN) / ωB97xD / 6–311 + G (2df, p)// CPCM (ACN) / ωB97xD / 6–31 + G (d,p)
M3 = CPCM (ACN) / ωB97xD / aug–cc–pvtz//CPCM (ACN) / ωB97xD / 6–31 + G (d,p)
M4 = CPCM (ACN) / M06–2X / aug–cc–pvtz // CPCM (ACN) / ωB97xD / 6–31 + G (d,p)
M5 = CPCM (ACN) / B2PLYP–D3 / aug–cc–pvtz // CPCM (ACN) / ωB97xD / 6–31 + G(d,p)
M6 = SMD (ACN) / B3LYP / 6–311 + G (2df,p) // SMD (ACN) / B3LYP / 6–31 + G (d,p)
M7 = CPCM (ACN) / ωB97xD / 6–311 + G (2df,p) // SMD (ACN) / B3LYP / 6–31 + G (d,p)
M8 = CPCM (ACN) / ωB97xD / aug–cc–pvtz // SMD (ACN) / B3LYP / 6–31 + G (d,p)
M9 = CPCM (ACN) / M06–2x / aug–cc–pvtz // SMD (ACN) / B3LYP / 6–31 + G (d,p)
M10 = CPCM (ACN) / B2PLYP–D3 / aug–cc–pvtz // SMD (ACN) / B3PLYP / 6–31 + G (d,p)

M11 = SMD (ACN) / ωB97xD / aug–cc–pvtz // SMD (ACN) / B3PLYP / 6–31 + G (d,p)
M12 = SMD (ACN) // M06–2X / aug–cc–pvtz // SMD (ACN) / B3PLYP / 6–31 + G (d,p)
M13 = SMD (ACN) / B2PLYP–D3 / aug–cc–pvtz // SMD (ACN) / B3PLYP / 6–31 + G (d,p)
M14 = SMD (ACN) / B3PLYP / 6–311 + G (2df,p) // SMD (ACN) / B3PLYP / 6–31 + G (d,p)
M15 = SMD (ACN) / B3LYP–GD3 / 6–311 + G (2df,p) // SMD (ACN) / B3LYP–GD3 / 6–31 + G (d,p)
M16 = SMD (ACN) / B3LYP–GD3 / 6–311 + G (2df,p) // SMD (ACN) / B3LYP–GD3 / 6–31 + G (d,p)
M17 = CPCM (ACN) / ωB97xD / aug–cc–pvtz // ωB97xD / 6–31 + G (d,p)
M18 = CPCM (ACN) / M06–2X / aug–cc–pvtz // ωB97xD / 6–31 + G (d,p)
M19 = CPCM (ACN) / B2PLYP–D3 / aug–cc–pvtz // ωB97xD / 6–31 + G (d,p)
M20 = CPCM (ACN) / M06–2X / 6–31 + G (d,p) // M06 – 2X / 6–311 + + G (2df, 2pd) // M06–2X / 6–31 + G (d,p)
M21 = CPCM (ACN) / M06–2X / 6–31 + G (d,p) // M06–2X / aug–cc–pvtz // M06–2X / 6–31 + G (d,p)
M22 = CPCM (ACN) / M06–2X / 6–31 + G (d,p) // M06–2X / aug–cc–pvtz // M06–2X / cc–pvdz
M23 = SMD (ACN) / M06–2X / 6–31 + G (d,p) // M06–2X / aug–cc–pvtz // M06–2X / cc-pvdz
M24 = SMD (ACN) / M06–2X / 6–31 + G (d,p) // MP2 / 6–311 + G (2df, p) // M06–2X / cc–pvdz
M25 = IPCM (ACN) / B3LYP / 6–311 + G (d,p) // MP2 / 6–311 + G (2df,p) // B3LYP / 6–31G(d)

RESULTS AND DISCUSION

For this work, we have selected a set of non-metallic hydride donors (Figure 1) and calculated their $\Delta G^*_{HHR}(AH^-)$ with 25 different computational models. The chosen set spans the experimental hydricity range of 26–129 kcal mol^{-1}.

Within the employed models, M1 and M3 are comparable to Lee's small and large models,[15] except that aug–cc–pVTZ was used instead of the def2–TZVP basis set in line with our recent results.[36] In addition to ωB97xD, M06–2X, and B3LYP functionals were used for optimizations as they were designed with different treatments of dispersion interactions. Apart from the ωB97xD functional, which includes Grimme's D2 correction, the dispersion interactions are partially incorporated into M06–2X through parametrization, while the B3LYP does not account for dispersion in any form. Our initial attempts to optimize structures using Gaussian16 employing Muckermann's approach failed, resulting in C–H dissociation in many instances. Additionally, UAHF radii should be avoided because they were optimized for HF/6–31G(d) method.[37,38] Therefore, the B3LYP approaches used here (M6-M16) employs the SMD solvation model instead of PCM / UAHF. Full details for all models are provided in the Computational details section.

The calculation of the hydricities was based on Eq. (3) – Eq. (5) given below, which correspond to equations (2, 4C, and 6) from the Ref. [12].

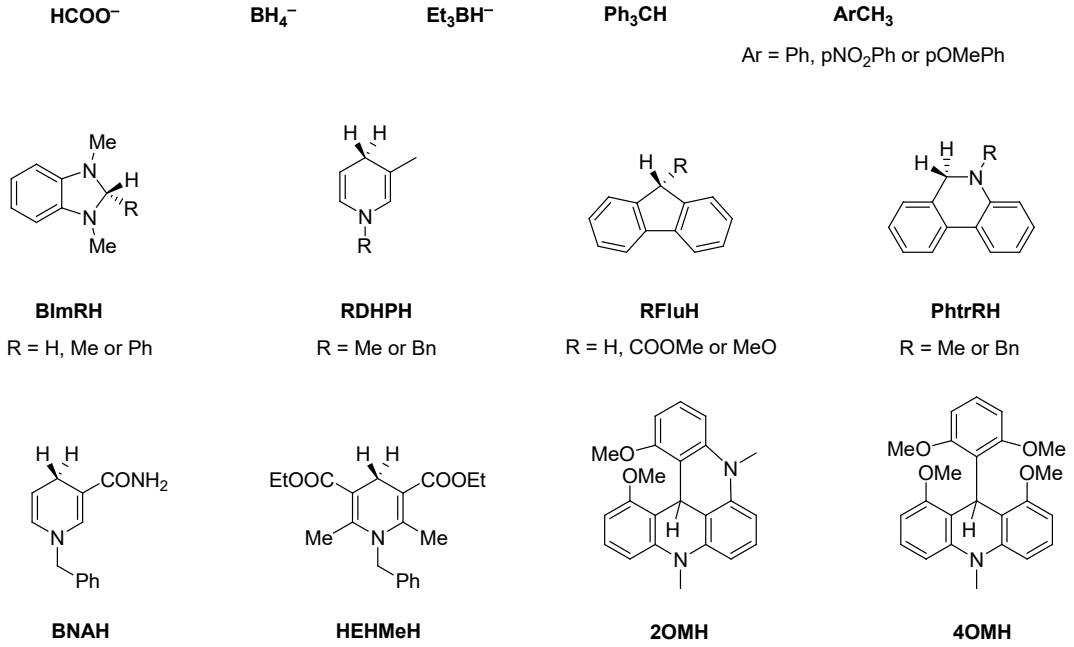


Figure 1. Structures of the hydride donors used in this work.

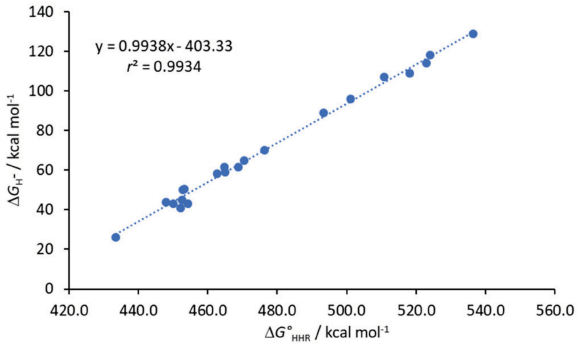


Figure 2. The correlation line obtained using the computational model M3 on 21 selected hydride donors.

$$\Delta G^*_{H}\text{-}(BH) = G°([B\text{-}H]^+) - G°(B) + \Delta G^*_{H}\text{-} \quad (3)$$

$$\Delta G^*_{HHR}(BH) = \Delta G°_{HHR}(BH) = G°([B\text{-}H]^+) - G°(BH) \quad (4)$$

$$\Delta G^*_{H}\text{-}(BH) = a \times \Delta G°_{HHR}(BH) + b \quad (5)$$

Equation (5) is the linear fit function that corrects systematic errors originating from the employed computational model, and the intercept "*b*" also contains the information about $\Delta G^*(H^-)$. It should also be emphasized that the equation $\Delta G^*_{HHR}(BH^-) = \Delta G°_{HHR}(BH^-)$ holds because the reference state correction factor ($\Delta G°\rightarrow*$) of 1.89 kcal mol^{-1} cancels out. The correlation obtained with model M3 is shown in Figure 2, and the computed $\Delta G°_{HHR}$ values for the selected models are given in Table 1. The correlation data for all models are presented in Table 2.

Compared with the pK_a calculations, the slopes of the regression lines are closer to the ideal value of 1, and the correlation coefficients are higher.[17] The MUE values range from 1.6 to 2.9 kcal mol^{-1}, corresponding to a ΔpK_a of 1.5, although the maximum deviation of the calculated values from the experimental ones is typically larger than 5 kcal mol^{-1}.

The best results were obtained with methods based on the B2PLYP-D3 and ωB97xD functional and the CPCM solvation approach (M1–M3 and M5). Slightly lower MAX values were obtained for the B2PLYP-D3 approaches, with RDHPH structures being the strongest offliners. Interestingly, the M06–2X approach (M4) proved to be inferior even to the M1 method. The results obtained for the methods M1–M5 indicate weak dependence of the correlation coefficient and other statistical parameters on the basis set size. The regression line obtained by the M1 method is compared to that obtained by Lee and coworkers.[15] The slope is significantly closer to 1 (the ideal value), and the intercept is higher (–405.5 against –476.22 in Lee's paper). It should be noted that Lee's correlation was constructed from the data obtained for 5 structures. When calculating the hydricities for our set of hydride donors using their

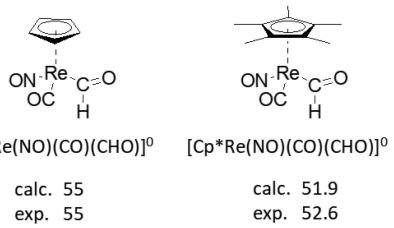


Figure 3. Comparison of the hydricities calculated for Rhenium complexes [CpReNO(CO)(CHO] and [Cp*ReNO(CO)(CHO] with M1 model with the experimental data.[15]

linear fit function (y = 1.1489 x – 476.22),[15] MUE rises to 4.0 kcal mol^{-1}, and MAX values for fluorene derivatives HFluH and MeOOCFluH exceed 10 kcal mol^{-1}. Conversely, fitting the calculated ΔG^*_{HHR} for two rhenium complexes to our scheme (Figure 3) yielded an excellent estimate of their hydricities with a deviation below 1 kcal mol^{-1}. In other words, we consider the computational model used by Lee and coworkers to be an excellent choice, but the linear fit function should have been created against the larger set of reference compounds.

As the next step, we compared the performance of CPCM and SMD solvation models (models M6–M16). In these cases, B3LYP/6-31+G(d,p) optimized geometries were used, while single-point energy calculations were systematically varied to assess the influence of the functional, basis set, and solvation model. The statistical data presented in Table 2 suggest the superior performance of the B2PLYP-D3/CPCM approach (M10), with wB97xD/CPCM (M8) being only marginally less accurate. Switching from CPCM to SMD in combination with either of these two functionals decreases the r^2 value and increases the MUE and MAX values, as indicated by the comparison of the methods M8 and M10 with M11 and M13, respectively. A comparison of the statistical data indicates that the B2PLYP-D3 approach is more sensitive to the changes in the solvent model.

The poorest correlations were obtained when the B3LYP (M14–M16) functional was used for single-point calculations, especially in combination with SMD as the solvent model. In these cases r^2 value drops significantly below 0.99. Two borane derivatives are the main outliers deviating by more than 7 kcal mol^{-1} from the correlation line. To test whether the dispersion correction affects the results, the models M15 and M16 were designed to incorporate Grimme's D3 correction explicitly during singlepoint energy calculations (M15) or at both stages (M16). Even then, the difference between the calculated and the experimental values for BH_4^- and Et_3BH^- remains between 7.4 and 8.8 kcal mol^{-1}. The results indicate that the B3LYP/SMD combination should be avoided for calculating hydricities.

Table 1. Hydricities of the selected set of hydride donors calculated with the selected computational model.[a]

BH	ΔG^{*}_{H-} / kcal mol^{-1}							
	Exp	M1	M3	M4	M5	M13	M19	M25
$HCOO^-$	44	45.5	41.6	41.6	43.1	44.1	43.6	41.3
BH_4^-	50.4	44.6	47.2	43.2	48.3	56.1	48.7	22.0[b]
BEt_3H^-	26	26.1	27.6	27.3	29.4	34.6	29.7	28.4
Ph_3CH	96	94.7	95.3	94.6	93.4	94.2	93.6	94.3
$PhCH_3$	118	116.6	117.2	116.7	118.9	118.0	119.2	117.5
pNO_2PhCH_3	129	129.8	129.7	129.2	131.5	131.0	131.0	128.5
$pOMePhCH_3$	107	105.0	104.8	104.6	106.0	106.3	105.9	106.2
BImHH	45	46.3	46.0	46.4	47.0	45.2	47.1	46.2
BImMeH	43	43.1	42.7	43.2	44.0	42.5	43.9	44.0
BImPhH	50	47.1	46.7	47.3	47.4	46.1	47.3	47.3
MeDHPH	41	44.8	45.9	46.4	45.0	43.6	43.8	42.6
BnDHPH	43	47.2	48.0	49.0	46.7	43.7	47.2	46.0
HFluH	109	111.2	111.6	111.3	110.8	111.9	111.0	111.6
MeOOCFluH	114	115.6	115.6	115.9	114.1	114.0	114.5	115.3
MeOFluH	89	88.1	87.2	87.8	88.0	88.8	88.0	89.6
PhtrMeH	61.4	62.5	62.2	62.1	61.4	61.3	61.5	62.4
PhtrBnH	64.8	64.5	64.2	64.0	63.1	63.5	62.9	63.8
BNAH	59	58.4	58.7	59.3	58.0	55.7	58.2	55.3
HEHMeH	61.5	60.9	60.0	60.2	60.4	56.8	59.6	59.0
2OMH	58.2	56.8	56.8	57.0	53.6	53.7	53.9	58.9
4OMH	70.2	70.5	70.8	72.6	69.2	68.6	69.2	70.9
	slope (a)	0.997	0.996	0.975	1.032	1.060	1.033	0.935
	inter. (b)	–405.5	–404.1	–394.2	–415.7	–423.3	–416.3	–369.7
	r^2	0.995	0.994	0.991	0.994	0.989	0.995	0.996
	MUE	1.6	1.8	2.1	1.8	2.2	1.8	1.6
	MAX	5.8	5.0	7.2	4.6	8.6	4.2	3.7
	RMSE	2.2	2.2	2.8	2.2	3.1	2.2	1.9

[a] All data are in kcal mol^{-1}; The experimental data were taken from the Ref. [13]; The largest outliers are marked in red; MUE and MAX stand for the "mean unsigned error" and "maximal absolute error".
[b] Excluded from the correlation.

Using the gas-phase geometries (M17–M19) leads to results similar to those obtained for the CPCM-optimized structures (M1–M5). Again, a slight deterioration of the correlation data was observed when the M06–2X functional was used instead of ωB97xD or B2PLYP–D3. The r^2 value decreases from 0.994 to 0.991, while the MUE and MAX values rise from 1.8 and 4.2 (or 5.6 for the ωB97xD) to 2.1 and 7.1 kcal mol^{-1}, respectively. While these changes seem small, they are larger than those caused by the difference in the optimization approach. A comparison of the M4, M9, M12, and M18 data shows that M06–2X is more tolerant to the choice of solvation model, regardless of which one is used. Although switching from the CPCM to the SMD solvation approach decreases MAX by > 1.0 kcal mol^{-1}, the overall correlation is not significantly affected, meaning that the errors are more equally distributed.

The models M20–M24 were employed as additional tests of the performance of the M06–2X functional. However, neither of these models was successful. The results obtained for model M24 were particularly disappointing, being among the worst ones with the poorest statistical parameters.

Table 2. Correlation data obtained for all 25 models used in this work.

	Method[a]	slope	intercept	r^2	MUE	MAX	RMSE
Optimization: ωB97xD(CPCM=ACN)/6–31+G(d,p)							
Single point (CPCM=ACN)BS1=6–311+G(2df,p), BS2 = auq–cc–pVTZ							
M1	ωB97xD/6–31+G(d,p)	0.997	–405.5	0.995	1.6	5.8	2.2
M2	ωB97xD/BS1	0.994	–403.9	0.994	1.8	5.2	2.3
M3	ωB97xD/BS2	0.996	–404.1	0.994	1.8	5.0	2.2
M4	M06–2X/BS2	0.975	–394.2	0.991	2.1	7.2	2.8
M5	B2PLYP–D3/BS2	1.032	–415.7	0.994	1.8	4.6	2.2
Optimization: B3LYP(SMD=ACN)/6–31+G(d,p)							
Single point (CPCM=ACN)BS1=6–311+G(2df,p), BS2 = auq–cc–pVTZ							
M6	B3LYP/BS1	1.060	–432.2	0.991	2.3	5.1	2.8
M7	ωB97xD/BS1	0.998	–405.8	0.994	1.8	5.3	2.3
M8	ωB97xD/BS2	1.000	–406.1	0.994	1.8	5.2	2.3
M9	M06–2X/BS2	0.977	–395.2	0.991	2.2	7.5	2.8
M10	B2PLYP–D3/BS2	1.035	–417.3	0.994	1.9	4.6	2.3
Single point (SMD = ACN)							
M11	ωB97xD/BS2	1.026	–413.2	0.991	2.2	6.7	2.8
M12	M06–2X/BS2	1.008	–404.3	0.992	2.2	6.1	2.6
M13	B2PLYP–D3/BS2	1.060	–423.3	0.989	2.2	8.6	3.1
M14	B3LYP/BS1	1.084	–437.8	0.985	2.9	8.8	3.6
M15	B3LYP–GD3/BS1	1.090	–441.4	0.987	2.6	7.6	3.4
M16	B3LYP–GD3/BS1[b]	1.083	–437.8	0.987	2.7	8.3	3.4
Optimization: ωB97xD(gas phase)/6–31+G(d,p)							
Single point (CPCM = ACN), basis set = auq–cc–pVTZ							
M17	ωB97xD	0.997	–404.6	0.994	1.8	5.6	2.2
M18	M06–2X	0.976	–394.5	0.991	2.1	7.1	2.8
M19	B2PLYP–D3	1.033	–416.3	0.995	1.8	4.2	2.2
Optimization: M06–2X(gas phase), BS1=6–31+G(d,p), BS2 = cc–pVDZ							
Single point (M06–2X/auq–cc–pVTZ or MP2/6–311+(2df,p), gas phase)							
Solvation (CPCM or SMD)							
M20	CPCM//M06–2X(big)//BS1	0.966	–390.0	0.991	2.1	7.4	2.8
M21	CPCM//M06–2X//BS1	0.971	–392.1	0.991	2.1	7.5	2.7
M22	CPCM//M06–2X//BS2	0.971	–391.9	0.990	2.2	7.7	2.9
M23	SMD//M06–2X//BS2	1.000	–400.7	0.991	2.3	5.9	2.8
M24	SMD//MP2//BS2	0.960	–375.3	0.986	2.5	10.9	3.5
Solvation (IPCM)							
M25	[c]	0.935	–369.7	0.996	1.6(1.6)	3.7 (28.4)	1.9 (6.5)

[a] The differences between the methods are emphasized. Full description of models M1–M25 is given in Computational details.
[b] Structures were optimized using B3LYP-D3(SMD=ACN)/6-31+G(d,p) approach.
[c] The data for BH_4^- were removed from the set. The values in parentheses were obtained for the full set, see the Discussion section.

Finally, model M25 was employed as a separate test case. This approach previously proved to be very good in predicting pK_a in acetonitrile,[17] and we wanted to test its performance in calculating hydricities. The model failed to properly interpret the hydricity of the borohydride anion ($BH4^-$), presumably due to inaccurate solvation energies obtained by the IPCM method. However, when borane $BH4^-$ was excluded, the data for 20 non-boronic hydride donors correlated well, with the largest deviation of 3.7 kcal mol^{-1} obtained for the BNA derivative. Other statistical parameters (r^2, MUE, and RMSE) are also superior to those obtained for other models, supporting its potential use, albeit with due care.

Gibbs Energy of the Anion in Acetonitrile

A few years ago, we suggested that if pK_a values are calculated using several model chemistries, the obtained slopes and intercepts can be used to estimate the Gibbs energy of proton in the given solvent.[17] The same concept is expected to be valid here for estimating $\Delta G^*(H^-)$. Briefly, Eq. (5) describes the relationship between $\Delta G^*_H{}^-(BH^-)$ and $\Delta G°_{HHR}(BH^-)$ where, in the ideal case, a = 1 and $b = \Delta G^*(H^-)$ giving Eq. (3). The current continuum solvation models are relatively simple, approximate approaches that usually give slopes and intercepts that differ from ideal values due to the inherent systematic errors. As we showed in our earlier paper, the intercepts and slopes show correlation across the different methods. Although $\Delta G^*(H^-)$ was not directly calculated, its linear dependence on the slopes of models M1–M25 is clearly visible (Figure 4).

In other words, Eq. (5) can be rewritten Eq. (6).

$$\Delta G^*_H\text{-}(BH^-) = a \times \Delta G°_{HHR}(BH^-) + a \times \Delta G^*(H^-) + c \qquad (6)$$

where the intercept b is expressed as a function of the slope Eq. (7), with an offset value c introduced as an additional parameter.

$$b = a \times \Delta G^*(H^-) + c \qquad (7)$$

The function presented in Figure 4 clearly confirms the necessity of the parameter c, but the further analysis of its possible physical meaning is beyond the scope of this paper. By interpolating the intercept to the slope of exactly 1, we obtained $\Delta G^*(H^-)_{ACN}$ of –403.1 kcal mol^{-1}. This result is in excellent agreement with the values of –400.7, –402.9 and –404.7 kcal mol^{-1} obtained previously.[39–41] This result, together with our previous results on the $\Delta G^*(H^+)_{ACN}$,[17] also confirms the correctness of our approach.

The same analysis was also conducted after separating the models into two subsets: CPCM–based and SMD/IPCM–based ones (see Section S2 in the Supporting Information). The estimated $\Delta G^*(H^-)_{ACN}$ values amount to –405.0 (CPCM) and –398.7 kcal mol^{-1} (SMD / IPCM). The results again show the somewhat poorer performance of the SMD-based models, as the obtained $\Delta G^*(H^-)_{ACN}$ value is underestimated relative to the experimental values by 2–6 kcal mol^{-1}, while the result for the CPCM based subset fall within the experimental data range with the absolute deviations between 0.3 and 2.4 kcal mol^{-1}.

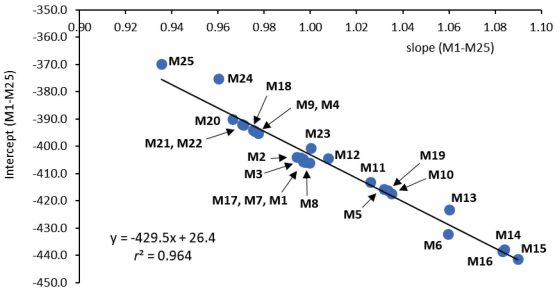


Figure 4. Correlation of the intercepts against slopes according to Eq. (7). The data are taken from Tables 1 and 2.

The error in the calculated $\Delta G^*(H^-)_{ACN}$ is estimated to be 10.2 kcal mol^{-1}. This estimation is based on the standard errors determined for the intercept value of each linear regression line, which range between 6.5 and 14.5 kcal mol^{-1}. The estimated error is not highly sensitive to the removal of any particular model; removing the three worst and three best models results in estimated errors of 9.6 and 10.5 kcal mol^{-1}, respectively.

CONCLUSION

The results presented in this work provide a deeper insight into the quality of the selected DFT approaches in estimating hydricity of the non-metallic hydride donors. Although very good results have been obtained earlier by others,[12,13,15] our results bring an additional analysis of the importance of optimization of the geometry in solution and performance of the SMD solvation approach, which is nowadays considered as the best continuum solvation model.

Most of the methods used here provided very good correlations with r^2 values above 0.99, but the maximal deviations go above 5.0 kcal mol^{-1}, which is quite large. The variant of Lee's approach[15] using ωB97xD coupled with the CPCM solvation approach performed slightly better than M06–2X, while we would not recommend the usage of B3LYP–based models. In general, neither optimization in solution nor changes in basis sets increased the quality of correlations to a large extent. By employing the correlation data obtained with various computational models, we estimated the Gibbs energy of the hydride ion in acetonitrile ($\Delta G^*(H^-)_{ACN}$) to be –403.1 ± 10.2 kcal mol^{-1}. The

excellent agreement with the literature data additionally supports our proposed approach, although the uncertainty is quite large.

We expect that the results will help the scientific community to develop new hydride donors, which is extremely important in the context of the modern need for efficient and recyclable CO_2-reducing agents.

Acknowledgment. The authors acknowledge funding by the Croatian Science Foundation, grants No. IP-2022-10-4385 (Spatial modulations of guanidines, SPACE-G) and IP-2024-05-7730 (Bis-phosphines as Metal-Free Catalysts for Small Molecules' Activation - Design and Synthesis, CatDesSyn). This research was performed using the Advanced computing service provided by the University of Zagreb Computing Centre – SRCE (Padobran cluster).

Supplementary Information. Supporting information to the paper is attached to the electronic version of the article at: https://doi.org/10.5562/cca4247.

PDF files with attached documents are best viewed with Adobe Acrobat Reader which is free and can be downloaded from Adobe's web site.

REFERENCES

[1] M. B. Smith, *Reduction* (Ch. 4) in *Organic Synthesis*, *3rd Ed.*, Academic Press, Cambridge, USA, **2010**, pp. 347-490. https://doi.org/10.1016/B978-1-890661-40-3.50004-1

[2] M. S. Jeletic, M. T. Mock, A. M. Appel, J. C. Linehan, *J. Am. Chem. Soc.* **2013**, *135*, 11533–11536. https://doi.org/10.1021/ja406601v

[3] S. E. Clapham, A. Hadzovic, R. H. Morris, *Coord. Chem. Rev*. **2004**, *248*, 2201–2237. https://doi.org/10.1016/j.ccr.2004.04.007

[4] R. M. Bullock, *Chem. Eur. J*. **2004**, *10*, 236–2374. https://doi.org/10.1002/chem.200305639

[5] C. Zheng, S.-L. You, *Chem. Soc. Rev.* **2012**, *41*, 2498–2518. https://doi.org/10.1039/c1cs15268h

[6] S. Ilic, J. L. Gesiorski, R. B. Weerasooriya, K. D. Glusac, *Acc. Chem. Res.* **2022**, *55*, 844-856. https://doi.org/10.1021/acs.accounts.1c00708

[7] T. Harada, S. Murakami, R. Matsubara, *Tetrahedron Chem* **2025**, *16*, 100147. https://doi.org/10.1016/j.tchem.2025.100147

[8] E. S. Wiedner, M. B. Chambers, C. L. Pitman, R. M. Bullock, A. J. M. Miller, A. M. Appel, *Chem. Rev*. **2016**, *116*, 8655−8692. https://doi.org/10.1021/acs.chemrev.6b00168

[9] X.-Q. Zhu, M. Zhang, Q.-Y. Liu, X.-X. Wang, J.-Y. Zhang, J.-P. Cheng, *Angew. Chem. Int. Ed.* **2006**, *45*, 3954 –3957. https://doi.org/10.1002/anie.200600536

[10] X.-Q. Zhu, M.-T. Zhang, A. Yu, C.-H. Wang, J.-P. Cheng, *J. Am. Chem. Soc*. **2008**, *130*, 2501–2516. https://doi.org/10.1021/ja075523m

[11] D. L. DuBois, *Inorg. Chem.* **2014**, *53*, 3935–3960. https://doi.org/10.1021/ic4026969

[12] J. T. Muckerman, P. Achord, C. Creutz, D. E. Polyansky, E. Fujita, *Procl. Nat. Acad Sci. (PNAS)* **2012**, *109*, 15657–15662. https://doi.org/10.1073/pnas.1201026109

[13] S. Ilic, A. Alherz, C. B. Musgrave, K. D. Glusac, *Chem. Soc. Rev*. **2018**, *47*, 2809–2836. https://doi.org/10.1039/C7CS00171A

[14] S. Ilić, U. Pandey Kadel, Y. Basdogan, J. A. Keith, K. D. Glusac, *J. Am. Chem. Soc*. **2018**, *140*, 4569–4579. https://doi.org/10.1021/jacs.7b13526

[15] J. Chen, H. Yu, D. Tan, R. Lee, *Chem. Commun*. **2023**, *59*, 5201–5204. https://doi.org/10.1039/D3CC00475A

[16] Z. Glasovac, M. Eckert-Maksić, Z. B. Maksić, *New J. Chem*. **2009**, *33*, 588–597. https://doi.org/10.1039/B814812K

[17] Z. Glasovac, B. Kovačević, *Int. J. Mol. Sci*. **2022**, *23*, 10576. https://doi.org/10.3390/ijms231810576

[18] A. Klamt, F. Eckert, M. Diedenhofen, M. E. Beck, *J. Phys. Chem. A* **2003**, *107*, 9380–9386. https://doi.org/10.1021/jp034688o

[19] F. Eckert, I. Leito, I. Kaljurand, A. Kütt, A. Klamt, M. Diedenhofen, *J. Comput. Chem*. **2009**, *30*, 799–810. https://doi.org/10.1002/jcc.21103

[20] Gaussian 16, Revision C.02, M. J. Frisch, G. W. Trucks, H. B. Schlegel, G. E. Scuseria, M. A. Robb, J. R. Cheeseman, G. Scalmani, V. Barone, G. A. Petersson, H. Nakatsuji, X. Li, M. Caricato, A. V. Marenich, J. Bloino, B. G. Janesko, R. Gomperts, B. Mennucci, H. P. Hratchian, J. V. Ortiz, A. F. Izmaylov, J. L. Sonnenberg, D. Williams-Young, F. Ding, F. Lipparini, F. Egidi, J. Goings, B. Peng, A. Petrone, T. Henderson, D. Ranasinghe, V. G. Zakrzewski, J. Gao, N. Rega, G. Zheng, W. Liang, M. Hada, M. Ehara, K. Toyota, R. Fukuda, J. Hasegawa, M. Ishida, T. Nakajima, Y. Honda, O. Kitao, H. Nakai, T. Vreven, K. Throssell, J. A. Montgomery, Jr., J. E. Peralta, F. Ogliaro, M. J. Bearpark, J. J. Heyd, E. N. Brothers, K. N. Kudin, V. N. Staroverov, T. A. Keith, R. Kobayashi, J. Normand, K. Raghavachari, A. P. Rendell, J. C. Burant, S. S. Iyengar, J. Tomasi, M. Cossi, J. M. Millam, M. Klene, C. Adamo, R. Cammi, J. W. Ochterski, R. L. Martin, K. Morokuma, O. Farkas, J. B. Foresman, and D. J. Fox, Gaussian, Inc., Wallingford CT, **2019**.

[21] J.-D. Chai, M. Head-Gordon, *Phys. Chem. Chem. Phys*. **2008**, *10* 6615-6620. https://doi.org/10.1039/b810189b

[22] Y. Zhao, D. G. Truhlar, *Theor. Chem. Acc*. **2008**, *120*, 215–241. https://doi.org/10.1007/s00214-007-0310-x

[23] A. D. Becke, *J. Chem. Phys.* **1993**, *98*, 5648–5652. https://doi.org/10.1063/1.464913
[24] C. Lee, W. Yang, R. G. Parr, *Phys. Rev. B* **1988**, *37*, 785–789. https://doi.org/10.1103/PhysRevB.37.785
[25] B. Miehlich, A. Savin, H. Stoll, H. Preuss, *Chem. Phys. Lett*. **1989**, *157*, 200–206. https://doi.org/10.1016/0009-2614(89)87234-3
[26] P. J. Stephens, F. J. Devlin, C. F. Chabalowski, M. J. Frisch, *J. Phys. Chem.* **1994**, *98*, 11623–11627. https://doi.org/10.1021/j100096a001
[27] S. Grimme, J. Antony, S. Ehrlich, H. Krieg, *J. Chem. Phys*. **2010**, *132*, 154104. https://doi.org/10.1063/1.3382344
[28] S. Grimme, S. Ehrlich, L. Goerigk, *J. Comp. Chem.* **2011**, *32*, 1456–1465. https://doi.org/10.1002/jcc.21759
[29] L. Goerigk, S. Grimme, *J. Chem. Theory Comput*. **2011**, *7*, 291–309. https://doi.org/10.1021/ct100466k
[30] C. Møller, M. S. Plesset, *Phys. Rev.* **1934**, *46*, 618–622. https://doi.org/10.1103/PhysRev.46.618
[31] M. J. Frisch, M. Head-Gordon, J. A. Pople, *Chem. Phys. Lett.* **1990**, *166*, 281–289. https://doi.org/10.1016/0009-2614(90)80030-H
[32] V. Barone, M. Cossi, *J. Phys. Chem. A* **1998**, *102*, 1995–2001. https://doi.org/10.1021/jp9716997
[33] M. Cossi, N. Rega, G. Scalmani, V. Barone, *J. Comp. Chem.* **2003**, *24*, 669–681. https://doi.org/10.1002/jcc.10189
[34] A. V. Marenich, C. J. Cramer, D. G. Truhlar, *J. Phys. Chem. B* **2009**, *113*, 6378–6396. https://doi.org/10.1021/jp810292n
[35] J. B. Foresman, T. A. Keith, K. B. Wiberg, J. Snoonian, M. J. Frisch, *J. Phys. Chem.* **1996**, *100*, 16098–16104. https://doi.org/10.1021/jp960488j
[36] Z. Glasovac, B. Kovačević, D. Margetić, *Molecules* **2026**, *31*, 1167. https://doi.org/10.3390/molecules31071167
[37] V. Barone, M. Cossi, J. Tomasi, *J. Chem. Phys.* **1997**, *107*,3210–3221. https://doi.org/10.1063/1.474671
[38] L. Xu, M. L. Coote, *J. Chem. Theory Comput.* **2019**, *15*, 6958–6967. https://doi.org/10.1021/acs.jctc.9b00888
[39] M. R. Nimlos, C. H. Chang, C. J. Curtis, A. Miedaner, H. M. Pilath, D. L. DuBois, *Organometallics* **2008**, *27*, 2715–2722. https://doi.org/10.1021/om701218x
[40] X. Yang, J. Walpita, D. Zhou, H. L. Luk, S. Vyas, R. S. Khnayzer, S. C. Tiwari, K. Diri, C. M. Hadad, F. N. Castellano, A. I. Krylov, K. D. Glusac, *J. Phys. Chem. B* **2013**, *117*, 15290–15296. https://doi.org/10.1021/jp401770e
[41] G. Kovács, I. Pápai, *Organometallics* **2006**, *25*, 820–825. https://doi.org/10.1021/om050726+